VFAST Transactions on Mathematics
http://vfast.org/journals/index.php/VTM@ 2024 ISSN(e): 2309-0022, ISSN(p): 2411-6343
Volume 12, Number 1, January-June, 2024 *pp: 280-289*

New Results for Riemann Solution of the Cargo-LeRoux Model by the Application of Flux-Limiter Schemes

Sidrah Ahmed[1*]

[1]Department of Mathematical and Social Sciences, Sukkur IBA University, Sukkur, Pakistan

Keywords: *Cargo-LeRoux model, van der Waals equation of state, Riemann problem, Flux limiter schemes.* ***Subject Classification***: *65N08, 35Qxx.*

Journal Info:
Submitted:
March 13, 2024
Accepted:
April 20, 2024
Published:
May 27, 2024

Abstract The Rienamm solution of the Cargo-LeRoux model has been recently introduced in [5] in which authors have found the exact solutions to the initial value problem. This work is the first attempt to apply numerical methods for the Cargo-LeRoux model. The higher-order flux limiter method used here to carry out the simulations holds the total variation diminishing property and gives smooth solutions in steep gradient regions. Various limiter functions that lead to different accuracy in numerical results are tested for the Riemann problem. The numerical investigations presented in this work can be used to review limiter-based TVD schemes extensively and to construct a class of highly efficient finite volume/ finite difference methods for such models.

***Correspondence Author Email Address:**
dr.sidrah@iba-suk.edu.pk
DOI: 10.21015/vtm.v12i1.1748

1 Introduction

Researchers have been interested in exploring the Riemann problem for many decades. This has been due to a large domain of applications of the Riemann problem related to atmospheric, aerodynamics, chemical sciences, traffic and transport modeling, and multi-phase flows. Selected reference books can be seen from [11, 22, 26, 30]. The Riemann problem first proposed by [19] is characterized as a coupled system of

quasi-linear hyperbolic partial differential equations with particular initial data that separates two states of physical variables. The two states compose a piece-wise constant function with a discontinuity point. This initial data discontinuous profile poses a major challenge to finding a well-defined solution to the system as the continuity of physical variables is no longer established. Owing to this, much research has been done that eventually developed a theory regarding solutions to Riemann's problem. Among these approaches, numerical techniques are well established, and researchers are still improving these with their applicability to new models.

The first detailed discussion on the solution to Riemann problems related to gas dynamics, saint vienent system, and blood flow model was established by Toro et al [30]]. A slightly different approach of changing state variables for finding the Riemann solution was then introduced by Pang et al [16]. Further developments include the solution to hyperbolic conservation laws with non-conservative terms such as (shallow water models, horizontal temperature gradient, and pressure gradient terms, etc see in [2, 23, 29]. A large number of contributions has been made in this context such as the incorporation of the entropy equation for pressure gradient models by Mahmood, [24], establishing important analysis related to the existence and uniqueness of the Riemann problem for one-dimensional isentropic and non-isentropic gas dynamic equation [6, 14], the modified Riemann solutions for MHD problems including magnetic field effects on elementary waves presented in [32], investigating Riemann solutions for radiating non-ideal flows [25] etc.

The drift flux model for two-phase flow was presented in [1], in which authors applied Lie group analysis and reduced the system to a set of ordinary differential equations. Several extensions of the drift flux model have been studied in the context of the Riemann problem recently [21, 23, 34]. The delta-shock wave, a generalization of the ordinary shock wave, was studied by Liu [13]. They investigated a one-dimensional relativistic string equation in Minkowski space to explore the interaction between elementary and delta waves. Another approach to finding self-similarity solutions was used in [8], in which authors applied the Lie group transformations to the non-ideal dusty gas model. The self-similarity zero-viscosity solutions were obtained by [9] with the same methodology of Lie group transformations.

Developing numerical methods for solving Riemann problems is more challenging because of complex wave interactions leading to oscillations in numerical solutions and the computational complexities of the numerical methods. These complexities are due to the dissipation and dispersion of solution that inevitably appears in numerical solutions because the solution combines several traveling waves. Hence, significant errors arise in numerical solutions as a natural feature of nonlinear hyperbolic conservation laws. Nonetheless, numerical schemes must be designed to capture all elementary waves accurately. Hence, higher-order accuracy schemes are much more reliable than low-order schemes to achieve accuracy but require additional treatment to ensure many other important properties like positivity preserving of physical variables. Plenty of literature is available regarding the development and analysis of numerical methods. Most applied numerical techniques include finite difference methods, finite volume methods, discontinuous Galerkin methods and machine learning algorithms see in [3, 18, 20, 31, 33].

This work is the first attempt to apply a numerical scheme for the Crago Laurex model in a one-dimensional case. The conservative TVD difference scheme has been chosen for this study. The central properties of the scheme include monotone, stability, and less dissipation, which can all be achieved by imposing the TVD criteria and using flux limiters. Hence, both higher-order stability and accuracy in smooth regions are achieved [27, 28].

The flux limiters play an important role in resolving the solution at steep gradients and turning points, which usually co-occur. Spurious oscillations due to numerical instabilities at turning points may result

in a violation of the fundamental physical properties of the model. Hence, conservative TVD difference schemes are a good choice for handling such issues. These schemes switch on the higher-order accuracy corrections in numerical solutions if the solution is not smooth enough in the region of a steep gradient. A class of conservative schemes has been developed for conservation laws, which are non-oscillatory at steep gradients and higher-order accurate in smooth regions [4, 12]. Such methods are known as high-resolution schemes, and one of these has been applied in this work.

The remaining sections are designed as follows. Section 2 composed the Cargo-Lauroux model and its eigen-structure. Section 3 is based on the formulation of the numerical method, starting with the introduction of certain notations, and also gives some important properties of a high-resolution scheme. Finally, the last section presents numerical solutions and discusses the results for cases taken from [5]. The test cases demonstrate the successful implementation of numerical schemes to capture the elementary and delta shock waves.

2 The Cargo-LeRoux model

The Cargo-LeRoux model is a nonlinear system of partial differential equations. Its conservation law form is given as below:

$$\begin{aligned} \rho_t + (\rho u)_x &= 0 \\ (\rho q)_t + (\rho q u)_x &= 0 \\ (\rho u)_t + \left(\rho u^2 + q\right)_x &= 0 \end{aligned} \tag{1}$$

Recent studies on this model include [7, 10, 17]. The main objective of this paper is to resolve the system numerically by incorporating a van der Waals gas pressure equation of state [15], written as

$$p = A\left(\frac{\rho}{1 - a\rho}\right)^{\gamma}. \tag{2}$$

In the above equation, the van-der Waals excluded volume is a so that the term $a\rho$ is positive and less than 1, and the adiabatic constant is γ which is usually in the range $[1, 2]$. The authors in reference paper [5] use $A = 0.5$ as a constant.

The following initial data characterize an initial value problem for this model:

$$\mathbf{w}(x, 0) = \begin{cases} \mathbf{w}_l = (\rho_l, q_l, u_l)^{tr}, & x < 0, \\ \mathbf{w}_r = (\rho_r, q_r, u_r)^{tr}, & x > 0. \end{cases} \tag{3}$$

Where tr stands for the standard notation of transport and $\mathbf{w}_l$ and $\mathbf{w}_r$, denote the vectors of constant values of state/primitive variables ρ, q, and u on the left and right sides of $x = 0$, respectively.

It is straightforward to write the conservation law as follows.

$$\frac{\partial \mathbf{W}}{\partial t} + \frac{\partial \mathbf{G}(\mathbf{W})}{\partial x} = 0, \quad -\infty < x < \infty, \quad t \geq 0 \tag{4}$$

with defining $\mathbf{W}$ and $\mathbf{G}$ as follows:

$$\mathbf{W} = \begin{pmatrix} \rho \\ \rho q \\ \rho u \end{pmatrix}, \text{ and } \mathbf{G}(\mathbf{W}) = \begin{pmatrix} \rho u \\ \rho q u \\ \rho u^2 + p + q \end{pmatrix}. \tag{5}$$

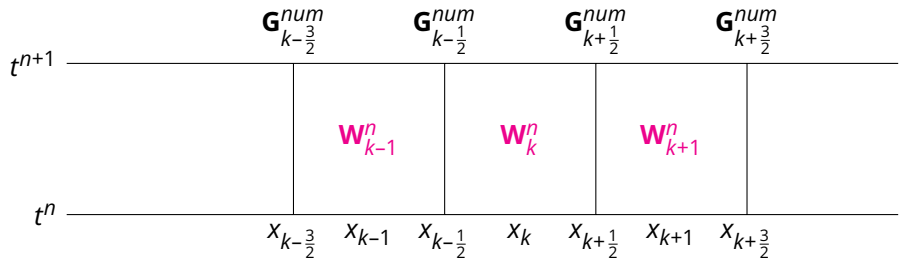

Figure 1. Schematic diagram showing Cells, time levels, cell centers and fluxes

Many researchers have changed the conservation law form for the vector of conserved variables $\mathbf{W} = \begin{pmatrix} \rho \\ \rho q \\ \rho u \end{pmatrix}$ to a new vector of variables $\mathbf{w} = \begin{pmatrix} \rho \\ q \\ u \end{pmatrix}$ and then deduced the expressions for the eigenvalues and eigenvectors. However, the standard approach of finding the eigenvalues from the conservation law model also gives the same expressions for the eigenvalues. Let $\mathbf{M} = \left[\frac{\partial \mathbf{W}}{\partial \mathbf{w}}\right]$ and $\mathbf{M} = \left[\frac{\partial \mathbf{w}}{\partial \mathbf{W}}\right]$ be the transformation matrices from conserved to primitive variables and vice versa. From equation 4 it follows that:

$$\begin{aligned} \frac{\partial \mathbf{W}}{\partial t} + \frac{\partial \mathbf{G}}{\partial \xi} &= 0 \\ \frac{\partial \mathbf{W}}{\partial t} + \frac{\partial \mathbf{G}}{\partial \mathbf{W}} \frac{\partial \mathbf{W}}{\partial \xi} &= 0 \\ \mathbf{M}\frac{\partial \mathbf{w}}{\partial t} + \mathbf{A}\mathbf{M}\frac{\partial \mathbf{w}}{\partial \xi} &= 0 \\ \mathbf{M}^{-1}\mathbf{M}\frac{\partial \mathbf{w}}{\partial t} + \mathbf{M}^{-1}\mathbf{A}\mathbf{M}\frac{\partial \mathbf{w}}{\partial \xi} &= 0 \\ \frac{\partial \mathbf{w}}{\partial t} + \mathbf{a}\frac{\partial \mathbf{w}}{\partial \xi} &= 0 \end{aligned} \tag{6}$$

Here the matrices $\mathbf{A}(\mathbf{W}) = \frac{\partial \mathbf{G}}{\partial \mathbf{W}}$ called the Jacobian matrix and the new matrix $\mathbf{a} = \mathbf{M}^{-1}\mathbf{A}\mathbf{M}$ are similar. The similar matrices have the same eigenvalues. These eigenvalues are obtained by solving the characteristic equation $\det(\mathbf{a} - \lambda \mathbf{I}) = 0$, for I to be a 3×3 identity matrix given as follows:

$$\lambda_1 = u - \sigma, \quad \lambda_2 = u \quad \text{and} \lambda_3 = u - \sigma, \tag{7}$$

where $\sigma = \sqrt{\frac{A\gamma\rho^{\gamma-1}}{(1-a\rho)^{\gamma+1}}} > 0$. It is readily seen that the eigenvalues are real and distinct, so the system 4 is strictly hyperbolic.

3 Numerical Scheme

A schematic diagram below illustrates the first step of a numerical method, which is a discretization of the domain. The notations in fig 1 are used as the discrete time steps t^{n+1}, spatial cell centers x_k, cell interfaces x_{k+1}, discrete values of conserved variables $\mathbf{W}^n_k$ and the numerical flux function $\mathbf{G}^{n,num}_k$.

Integration of equation 4 over the control volume $\left[x_{k-\frac{1}{2}}, x_{k+\frac{1}{2}}\right] \times \left[t^n, t^{n+1}\right]$ gives a discrete equation as

follows:

$$\begin{aligned}\mathbf{W}_k^{n+1} &= \int_{x_{k-\frac{1}{2}}}^{x_{k+\frac{1}{2}}} \frac{\mathbf{W}\left(x, t^{n+1}\right)}{\Delta x}\, \mathrm{d}x \\ &= \int_{x_{k+\frac{1}{2}}}^{x_{k+\frac{1}{2}}} \frac{\mathbf{W}\left(x, t^{n}\right)}{\Delta x}\, \mathrm{d}x + \frac{1}{\Delta x}\int_{t^n}^{t^{n+1}} \mathbf{G}\left(\mathbf{W}\left(x_{k-\frac{1}{2}}, \tau\right)\right) - \mathbf{G}\left(\mathbf{W}\left(x_{k+\frac{1}{2}}, \tau\right)\right) \\ &\approx \mathbf{W}_k^n + \frac{\Delta t}{\Delta x}\left(\mathbf{G}_{k-\frac{1}{2}}^{n,\,\mathrm{num}} - \mathbf{G}_{k+\frac{1}{2}}^{n,\,\mathrm{num}}\right).\end{aligned} \tag{8}$$

The numerical flux is a function of discrete values of conserved variables from neighboring cells, such as

$$\mathbf{G}_{k+\frac{1}{2}}^{n,num} = \mathbf{G}^{n,num}\left(\mathbf{W}_{k-p}^n, \ldots\ldots\ldots, \mathbf{W}_{k+q}^n\right). \tag{9}$$

Next, two more subscripts, *H* and *L*, differentiate the higher order from a lower order numerical flux. Hence, combined numerical flux is written as

$$\mathbf{G}_{k+\frac{1}{2}}^{n,num} = \mathbf{G}_{L_{k+\frac{1}{2}}}^{n,num} + \phi_k^n\left[\mathbf{G}_{H_{k+\frac{1}{2}}}^{n,num} - \mathbf{G}_{L_{k+\frac{1}{2}}}^{n,num}\right]. \tag{10}$$

The second term in 10 is an anti-diffusive term that effectively controls oscillation in steep gradient regions (see in [4, 12]). Lax Friedrich flux is selected as low order flux, i.e., $\mathbf{G}_{k+\frac{1}{2}}^{n,num}$ which gives the solution $\mathbf{W}_k^{n+1}$ below

$$\mathbf{W}_k^{n+1} = \frac{1}{2}\left(\mathbf{W}_{k+1}^n + \mathbf{W}_{k-1}^n\right) - \frac{\Delta t}{2\Delta x}\left(\mathbf{G}^{n,new}\left(\mathbf{W}_{k+1}^n\right) - \mathbf{G}^{n,new}\left(\mathbf{W}_{k-1}^n\right)\right). \tag{11}$$

while the higher order flux is coming from combining Lax Friedrichs and Lax Wendroff schemes see in [28]:

For one-space dimensions, the total variation diminishing TVD criteria is defined in terms of the total variation of the discrete values of the solution, i.e., $\sum_i(\mathbf{W}_{k+1}^n - \mathbf{W}_k^n)$ stated as below:

$$TV(\mathbf{W}^{n+1}) \leq TV(\mathbf{W}n). \tag{12}$$

The limiter function ϕ that appears in equation 10 plays the main role in forming a monotone TVD numerical scheme. It has been shown that ϕ taken as a function of special parameter *r* results in a non-oscillatory TVD scheme. This idea was first applied to non-linear conservation laws by Harten [4]. This parameter is usually taken as

$$r_k = \frac{\mathbf{W}_k^n - \mathbf{W}_{k-1}^n}{\mathbf{W}_{k+1}^n - \mathbf{W}_k^n}. \tag{13}$$

which is the check for local smoothness of the conserved variables. Hence, the limiter function controls the anti-diffusive correction relative to the magnitude of local non-smoothness appearing in the solution. Many researchers have introduced a class of flux-limiters schemes. For reference, see the table given below:

The results in this paper have been obtained using the minmod limiter.

4 Numerical Results

The discrete equation 4 in section 4 is applied to obtain the values of physical quantities ρ, potential *q*, and velocity *u* for different initial data sets. In this section, these test cases are now presented taken from [5].

Table 1. The flux-limiters of Sweby's TVD schemes.

Names	Flux Limiters Formula	Compressive or Diffusive
Superbee	$\phi(r) = \max[0, \min(2r, 1), \min(r, 2)]$	Compressive [27]
Van-Leer	$\phi(r) = (r + \|r\|)/(r + 1)$	Diffusive [27]
Minmod	$\phi(r) = \max[0, \min(r, 1)]$	Diffusive [27]
MUSCL	$\phi(r) = \max[0, \min(2r, \frac{r+1}{2}, 2)]$	Diffusive [27]

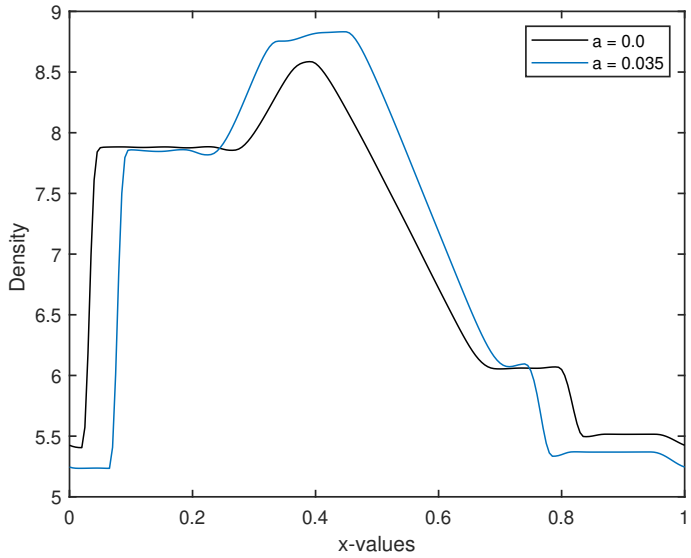

Figure 1. The plot for density ρ

.

4.1 Test-1

The initial data for this test is given as

$$\mathbf{w}(x,0) = \begin{cases} \mathbf{w}_l = (5.99924, 2.7996, 0.5975)^{tr}, & x < 0, \\ \mathbf{w}_r = (7.999242, 1.37452, -6.19633)^{tr}, & x > 0, \end{cases} \tag{14}$$

The solutions are shown in 4 and 3. Three different values of van der Waals excluded volume a used for plotting these results are $a = 0.0$ and $a = 0.035$. The constants A and γ equal 0.5 and 1.4, respectively. The domain length for the spatial variable x is 1.0, and the end time t equals 0.2.

Initially, the discontinuity is located at the mid-point of $x-axis$, but after time $t = 0; 2s$, it is seen that the discontinuity has evolved into a solution that is composed of a combination of elementary waves: a shock wave moving to the left, a contact discontinuity, and a rarefaction wave moving to the right. However, oscillations appear in the solution with an increase in value of a.

It is important to mention here that the results differ from those presented in [5]; however, the numerical values of quantities are compatible with the initial values.

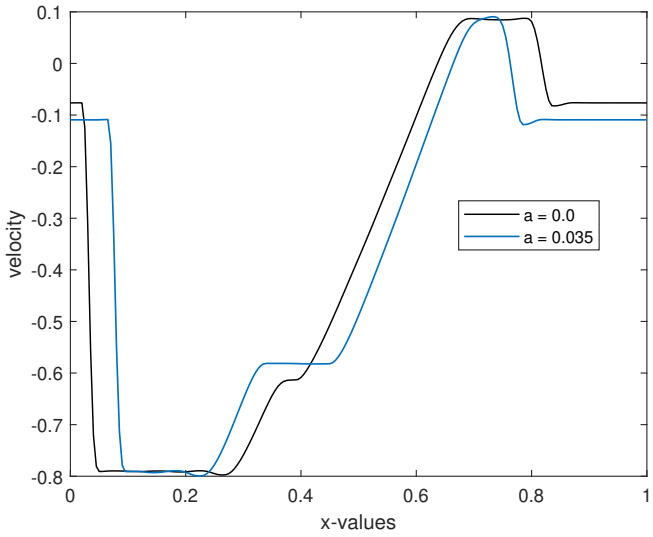

Figure 3. The plot for velocity v

.

4.2 Test-1

This test has been included to compare different flux limiters. The initial data for this test is given as

$$\mathbf{w}(x,0) = \begin{cases} \mathbf{w}_l = (0.96, 1.379, 1.0833)^{tr}, & x < 0, \\ \mathbf{w}_r = (1.7741, 1.5, 1.1187)^{tr}, & x > 0, \end{cases} \tag{15}$$

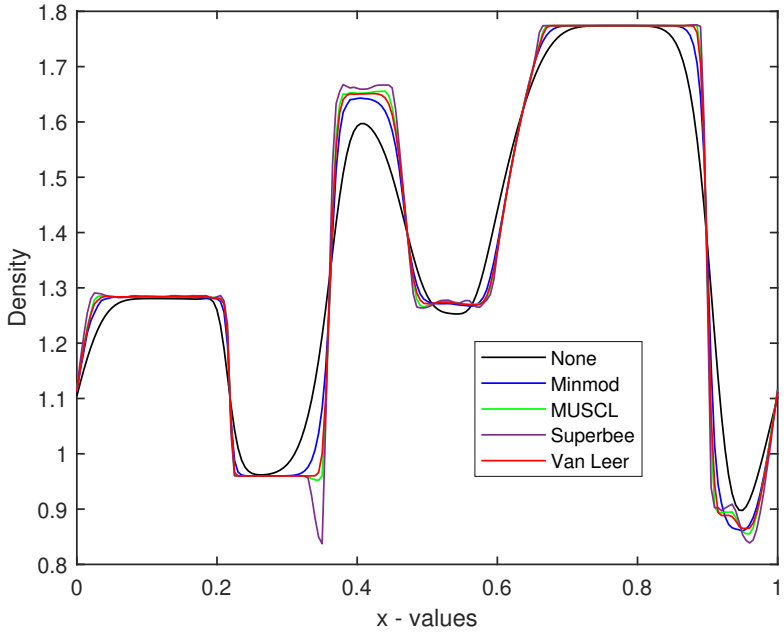

Figure 4. The plot for density ρ showing comparison of different flux limiters

.

The results for density are shown in the figure below. It is again observed that the solution profile does not exactly match the reference, however, the numerical values are within the range of the initial data and are compatible with those presented in the reference.

5 Conclusion and Future Work

The flux limiter methods are monotone and satisfy TVD properties. These are widely used in solving hyperbolic conservation laws. This work is based on the first numerical investigation of the Riemann problem for the Cargo-LeRoux model. The test cases show new results for this model. The examples from the literature are simulated with finite volume base flux limiter schemes. Although these results are still new to the given reference work, the work opens new lines to investigate this difference. It is planned to apply other numerical techniques such as physics-informed neural network methods and Weno algorithms.

Author Contributions

Sidrah Ahmed: Conceptualization, Methodology, Software, Writing- Original draft preparation, Visualization, Writing- Reviewing and Editing

Compliance with Ethical Standards

It is declared that this article does not contain any studies with human participants or animals performed by any of the authors.

Funding Information

No funding is available for this work so far.

Author Information

ORCID:

Sidrah Ahmed: 0000-0002-6493-7113

References

[1] Bira, B., Sekhar, T. R. and Zeidan, D. [2016], 'Application of lie groups to compressible model of two-phase flows', *Computers & Mathematics with Applications* **71**(1), 46–56.

[2] Dong, J. and Qian, X. [2022], 'Well-balanced and positivity-preserving surface reconstruction schemes solving ripa systems with nonflat bottom topography', *SIAM Journal on Scientific Computing* **44**(5), A3098–A3129.

[3] Du, Q., Glowinski, R., Hintermüller, M. and Süli, E. [2016], *Handbook of numerical methods for hyperbolic problems: basic and fundamental issues*, Elsevier.

[4] Harten, A. [1997], 'High-resolution schemes for hyperbolic conservation laws', *Journal of computational physics* **135**(2), 260–278.

[5] Jana, S. and Kuila, S. [2022], 'Exact solution of the flux perturbed riemann problem for cargo-leroux model in a van der waals gas', *Chaos, Solitons & Fractals* **161**, 112369.

[6] Jiang, W., Chen, T., Li, T. and Wang, Z. [2023], 'The riemann problem with delta initial data for the non-isentropic improved aw-rascle-zhang model', *Acta mathematica scientia* **43**(1), 237–258.

[7] Karna, A. K. and Satapathy, P. [2023], 'Lie symmetry analysis for the cargo–leroux model with isentropic perturbation pressure equation of state', *Chaos, Solitons & Fractals* **177**, 114241.

[8] Kim, Y. J. [2001], 'A self-similar viscosity approach for the riemann problem in isentropic gas dynamics and the structure of the solutions', *Quarterly of Applied Mathematics* **59**(4), 637–665.

[9] Kuila, S. and Sekhar, T. R. [2018], 'Interaction of weak shocks in the drift-flux model of compressible two-phase flows', *Chaos, Solitons & Fractals* **107**, 222–227.

[10] Kumozec, D. and Nedeljkov, M. [2024], 'The riemann problem for the generalized chaplygin gas with a potential', *Zeitschrift für angewandte Mathematik und Physik* **75**(2), 1–17.

[11] Lax, P. D. [1957], 'Hyperbolic systems of conservation laws ii', *Communications on pure and applied mathematics* **10**(4), 537–566.

[12] LeVeque, R. J. [2002], *Finite volume methods for hyperbolic problems*, Vol. 31, Cambridge University Press.

[13] Liu, J. and Liu, R. [2020], 'Riemann problem and wave interactions for the one-dimensional relativistic string equation in minkowski space', *Journal of Mathematical Analysis and Applications* **486**(2), 123932.

[14] Mondal, R. et al. [2024], 'On the interactions of arbitrary shocks in isentropic drift-flux model of two-phase flows', *The European Physical Journal Plus* **139**(1), 1–11.

[15] Pandey, M. and Sharma, V. [2007], 'Interaction of a characteristic shock with a weak discontinuity in a non-ideal gas', *Wave Motion* **44**(5), 346–354.

[16] Pang, Y. and Hu, M. [2019], 'The riemann problem for the one-dimensional compressible flow of a van der waals gas', *Zeitschrift für angewandte Mathematik und Physik* **70**(5), 142.

[17] Pradhan, P. K., Zeidan, D. and Pandey, M. [2023], 'Multi-dimensional optimal system and conservation laws for chaplygin gas cargo-leroux model', *Journal of Mathematical Analysis and Applications* **521**(1), 126912.

[18] Richtmyer, R. D. and Dill, E. [1959], 'Difference methods for initial-value problems', *Physics Today* **12**(4), 50–50.

[19] Riemann, B. [1860], *Über die Fortpflanzung ebener Luftwellen von endlicher Schwingungsweite*, Vol. 8, Verlag der Dieterichschen Buchhandlung.

[20] Roe, P. L. [1981], 'Approximate riemann solvers, parameter vectors, and difference schemes', *Journal of computational physics* **43**(2), 357–372.

[21] Shah, S., Singh, R. and Chaudhary, B. K. [2023], 'Concentration and cavitation of riemann solutions to two-phase chaplygin flows under vanishing pressure and flux approximation', *Communications in Nonlinear Science and Numerical Simulation* **118**, 107065.

[22] Sharma, V. D. [2010], *Quasilinear hyperbolic systems, compressible flows, and waves*, CRC Press.

[23] Shen, C. [2023], 'The transition of riemann solutions for the drift-flux model with the pressure law for the extended chaplygin gas', *Physics of Fluids* **35**(4).

[24] Sheng, W., Chen, H., Liu, Y. and Lai, G. [2023], 'The riemann problem of pressure gradient equations to the zeldovich–von neumann–doring combustion model for reacting flow', *Available at SSRN 4584923* .

[25] Singh, M. and Arora, R. [2021], 'Propagation of one-dimensional planar and nonplanar shock waves in nonideal radiating gas', *Physics of Fluids* **33**(4).

[26] Smoller, J. [2012], *Shock waves and reaction—diffusion equations*, Vol. 258, Springer Science & Business Media.

[27] Sweby, P. [1989], *Source terms and conservation laws: a preliminary discussion*, University of Reading. Department of Mathematics.

[28] Sweby, P. K. [1984], 'High-resolution schemes using flux limiters for hyperbolic conservation laws', *SIAM journal on numerical analysis* **21**(5), 995–1011.

[29] Thanh, N. X., Thanh, M. D. and Cuong, D. H. [2020], 'Godunov-type numerical scheme for the shallow water equations with horizontal temperature gradient', *Taiwanese Journal of Mathematics* **24**(1), 179–223.

[30] Toro, E. F. [2013], *Riemann solvers and numerical methods for fluid dynamics: a practical introduction*, Springer Science & Business Media.

[31] Xiong, F., Liu, L., Liu, S., Wang, H. and Yong, H. [2023], 'Gradient-weighted physics-informed neural networks for one-dimensional euler equation', *Authorea Preprints* .

[32] Xu, K., Gao, Z., Qian, Z. and Lee, C.-H. [2024], 'Exact ideal magnetohydrodynamic riemann solutions considering the strength of intermediate shocks', *Physics of Fluids* **36**(1).

[33] Xu, L., Liu, Z., Feng, Y. and Liu, T. [2024], 'Physics-constrained neural networks as multi-material riemann solvers for compressible two-gas simulations', *Journal of Computational Science* **78**, 102261.

[34] Yue, Y. and Guo, L. [2023], 'The special solutions of two-dimensional drift-flux equations for the two-phase flow', *Physics of Fluids* **35**(9).